

Satellite SST and SSS Observations and Their Roles to Constrain Ocean Models

Tong Lee¹ and Chelle Gentemann²

¹*Jet Propulsion Laboratory, California Institute of Technology, Pasadena, California, USA;* ²*Earth and Space Research, Seattle, Washington, USA*

Sea surface temperature (SST) and sea surface salinity (SSS) are important parameters of the ocean that influence ocean circulation, air-sea interactions, and biogeochemistry. In the past few decades, since SST measurements from space have become routine, they have been fundamental to ocean and climate research. In the past several years, satellite measurements of SSS have become available to strengthen research and applications for the oceans and the linkages with other elements of the Earth system. This chapter introduces the key principles and advantages of measuring SST and SSS from space, their complementarity use with other satellite and in situ observations, the past and current missions for these measurements, characteristics of uncertainties for the related data products, and the utility of these measurements in evaluating and constraining ocean model/assimilation systems and improving forecasts.

Importance of SST and SSS on Ocean and Air-sea Interaction Processes

Sea surface temperature (SST) and sea surface salinity (SSS) are important to ocean dynamics. These two parameters determine the surface density of the ocean. Surface density is essential to various ocean processes such as the formation of water masses at the ocean surface, ventilation, and mixed-layer dynamics. At high-latitude ocean where the vertical stratification is relatively weak, small variations in surface density due to SST and SSS changes can have significant impacts on vertical mixing and convection.

SST is a critical parameter for air-sea interactions. It affects the air-sea surface temperature difference, thereby contributing to local air-sea heat flux. Horizontal gradients of SST can also regulate ocean-atmosphere coupling, for example, through SST-wind feedback. A basin-scale example is the coupling of zonal SST gradients and zonal winds across the tropical Pacific Ocean associated with the El Niño-Southern Oscillation (e.g., Bjerknes 1969, Kumar and Hoerling, 1998). SST-wind coupling can also occur on smaller scales, such as those associated with tropical instability waves and ocean eddies (e.g., Chelton et al., 2001). SSS does not directly affect air-sea heat flux. However, it can influence SST and thus air-sea heat flux indirectly when there is SSS-related barrier layer (e.g., Lindstrom et al., 1987; Sprintall and Tomczak, 1992). The latter is a salinity-stratified layer within the isothermal layer. The barrier layer inhibits the vertical mixing

Lee, T., and C. Gentemann, 2018: Satellite SST and SSS observations and their roles to constrain ocean models. In "New Frontiers in Operational Oceanography", E. Chassignet, A. Pascual, J. Tintoré, and J. Verron, Eds., GODAE OceanView, 271-288, doi:10.17125/gov2018.ch11.

between the mixed layer above it and the thermocline beneath it, and thus indirectly affects SST and heat flux.

Given their importance in ocean and air-sea interaction processes, observations of SST and SSS and their use in ocean and coupled ocean-atmosphere model assimilation systems are central to the fidelity of the estimated ocean state as well as to ocean and coupled ocean-atmosphere forecasts across different timescales.

Advantages of Satellite SST and SSS and Complementarity with In situ Observations

Satellite and in situ measurements of SST and SSS are complementary to each other. Satellites provide more uniform spatiotemporal sampling than in situ systems to resolve oceanographic features. As such, they help monitor features with scales that are not resolved or adequately captured by in situ systems and they help decipher large-scale signals and smaller-scale features such as eddies and fronts. Additionally, satellites have synoptic coverage of coastal oceans, marginal seas, and high-latitude oceans, regions where in situ measurements are generally sparse. Satellite spatial sampling also enables the calculation of spatial derivative fields systematically, which is vital to studies of ocean dynamics and air-sea interaction. Moreover, synoptic coverage of global ocean SST and SSS by satellites facilitates the studies of large-scale teleconnections and impacts.

On the other hand, in situ SST and SSS measurements provide accurate ground truthing for calibration and validation of corresponding satellite measurements. In particular, the near-global Argo array and the tropical moored buoy array (TAO/TRITON, PIRATA, and RAMA) are important backbone datasets for evaluating and improving satellite retrievals of SST and SSS (Donlon et al., 2002; O'Carroll et al., 2008; Gentemann et al., 2004; Tang et al., 2014). High-frequency (e.g., hourly) measurements from moorings also help de-alias signals that may not be adequately sampled by satellites (e.g., diurnal signals). In situ measurements of temperature and salinity profiles are also important to the interpretation of satellite SST and SSS by providing measurements of the vertical structure. In addition, satellite and in situ data have been used synergistically to produce blended satellite/in situ products for SST (e.g., Reynolds et al., 2007) and SSS (e.g., Xie et al., 2014; Nardelli et al., 2016; Droghei et al., 2016). There have also been efforts that combined satellite SSS with the higher-resolution satellite SST to enhance the resolution of SSS products using multifractal fusion methods (e.g., Umbert et al., 2013; Olmeda et al., 2016).

Satellite Observations of SST

Satellite SST observing systems have decades of history. The first satellite program that measured SST was the TIROS weather satellite program in the late 1960s. The Advanced Very High Resolution Radiometers (AVHRR) onboard the NOAA series satellites from the early 1980s have brought the satellite SST observing system into a relatively mature stage for operational monitoring (Casey et al., 2010). There have been a series of technology advancements in satellite infrared (IR)

SST sensors, such as the European Space Agency's Along-Track Scanning Radiometer (ATSR) and Advanced Along-Track Scanning Radiometer (AATSR) (Llewellyn-Jones et al., 2001). Furthermore, a significant advancement in satellite SST observing systems has been the addition of passive microwave (PMW) sensors such as the Advanced Microwave Scanning Radiometer (AMSR) on JAXA's ADOES-II satellite (2002-2003), AMSR-E on the National Aeronautics and Space Administration's (NASA) EOS Aqua satellite (2002-2011) and AMSR-2 on JAXA's GCOM-W1 satellite (2012 onward) (Gentemann, 2014; Gentemann and Hilburn, 2015). International efforts have enabled a comprehensive constellation of SST-measuring satellites for past several years that will continue on into the next decade, both on polar and geostationary orbits (Figs. 11.1 and 11.2).

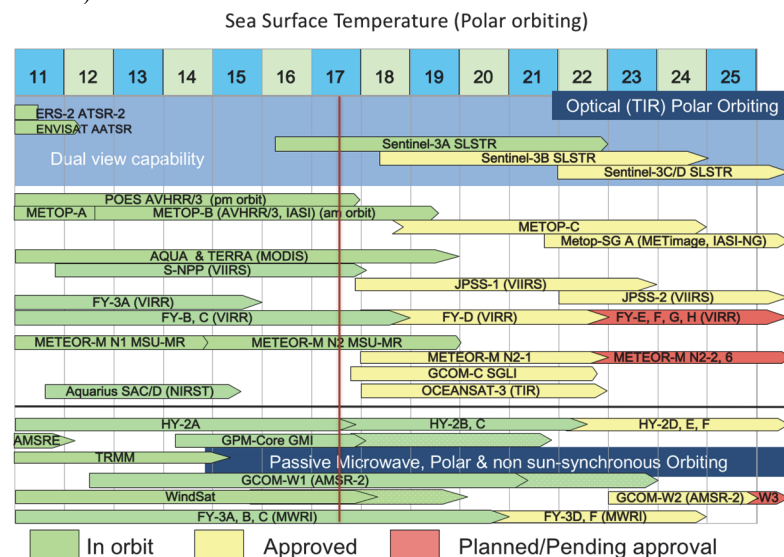


Figure 11.1. International constellation of polar-orbit SST satellites.

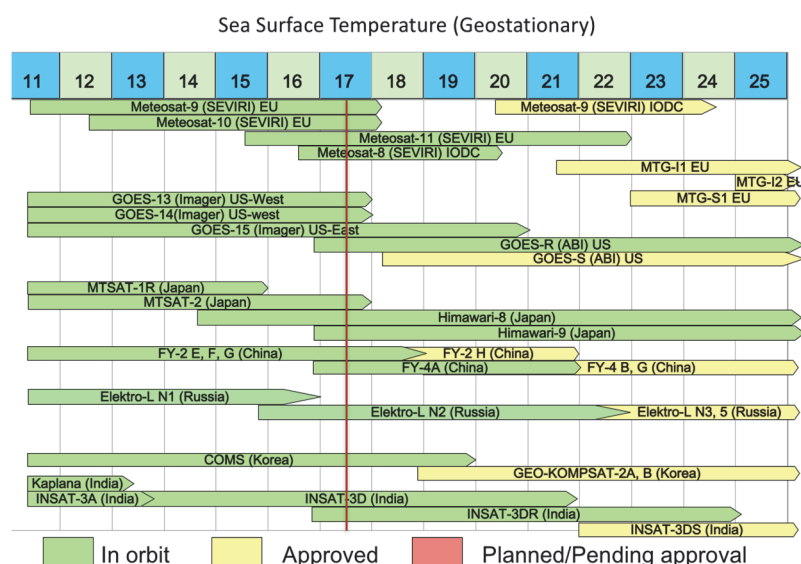


Figure 11.2. International constellation of geostationary SST satellites.

IR sensors measure SST in the top 10 microns of the ocean surface while PMW sensors measure SST in the top millimeters of the ocean, which can cause relative biases between IR and PMW SST especially due to diurnal heating and evaporative cooling, processes that are not well understood. This complicates the comparison and blending between IR and PMW SST. To address this, efforts have been made to convert the “skin SST” measured by IR and PMW sensors to “bulk SST” or “Foundation SST” (e.g., Reynolds et al., 2007; Donlon et al., 2007).

IR and PMW SST sensors have respective advantages and limitations. IR SST sensors have a long heritage and decades of service on record while PMW SST sensors have been in use for a much shorter time period (see above). IR SST sensors have much better spatial resolution (1-4 km) than PMW SST (~25 km). IR sensors are not able to measure SST through clouds and they are significantly affected by other atmospheric effects (e.g., water vapor and atmospheric aerosols). This is especially true for AVHRR-like single-view IR sensors. A large volcanic event could significantly impact the availability and accuracy of the IR SST (Reynolds, 1993). In comparison, PMW sensors can see through clouds and are relatively insensitive to atmospheric effects such as aerosols. However, PMW SST sensors are not able to retrieve SSTs near land or sea ice and they are influenced by rain, surface roughness, and radio frequency interference. The main source of radio frequency interference contamination is from reflected geostationary satellite transmissions, but satellite-to-satellite radio frequency interference is also a growing problem (Gentemann, 2014). A good graduate student-level resource that describes the differences between IR and PMW SST is <http://www2.hawaii.edu/~jmaurer/sst>, and the Group for High Resolution SST (GHRSST) Project (<https://www.ghrsst.org>) has produced a suite of high-resolution (< 10 km), level-4 SST products that synthesize SST observations from various satellites, some also including in situ SST measurements.

Salinity Remote Sensing: A New Frontier in Satellite Oceanography

Overview of satellite SSS missions

Three satellite missions have pioneered the measurements of SSS from space (Fig. 11.3). These are the Soil Moisture and Ocean Salinity (SMOS) Mission (2009-present) (Lagerloef and Font, 2010; Reul et al., 2012), the Aquarius/SAC-D Mission (June 2011-June 2015) (Lagerloef and Font, 2010; Lagerloef et al., 2013), and the Soil Moisture Active Passive (SMAP) Mission (January 2015-present) (Entekhabi et al., 2014; Tang et al., 2017). SMOS is a European Space Agency mission that measures both soil moisture and SSS. Aquarius/SAC-D is a joint mission between NASA and the Argentine National Space Activity Commission dedicated to SSS measurements. SMAP is a NASA mission with a main objective to measure soil moisture and the freeze/thaw state of the Earth. Even though SSS measurement is not one of the main objectives of the SMAP mission, the similarity in the designs of SMAP and Aquarius instruments allows SSS retrieval from SMAP. Likewise, soil moisture has also been retrieved from Aquarius even though the mission was dedicated to SSS measurements. In addition to soil moisture and SSS, thin sea ice thickness (up to

approximately 50 cm) has also been retrieved from the measurements of these L-band these satellites.

All three missions operate at L-band radiometric frequencies (approximately 1.4 GHz), a frequency band where the surface brightness temperature has overall good sensitivity to changes in soil moisture and SSS. L-band is also a protected frequency band reserved for astronomy observations, thereby minimizing radio frequency interference by radar signals on the Earth. Aquarius and SMAP both have an active-passive design with a L-band radar scatterometer integrated with the L-band radiometer. SMOS' design is passive L-band radiometry. All three satellites are on sun-synchronous polar orbits with high inclinations, allowing for full coverage of polar oceans.

SMOS has a 33 km spatial resolution with a 10-day repeat and a three-day sub-cycle. Aquarius has a 100-150 km spatial resolution and a seven-day repeat. SMAP has a 40 km spatial resolution and an eight-day repeat. Therefore, all three missions provide synoptic measurements of SSS over the global ocean with spatial scales much finer than those afforded by the Argo array, and they resolve higher-frequency signals (e.g., tropical instability waves) that are difficult to capture using Argo floats.

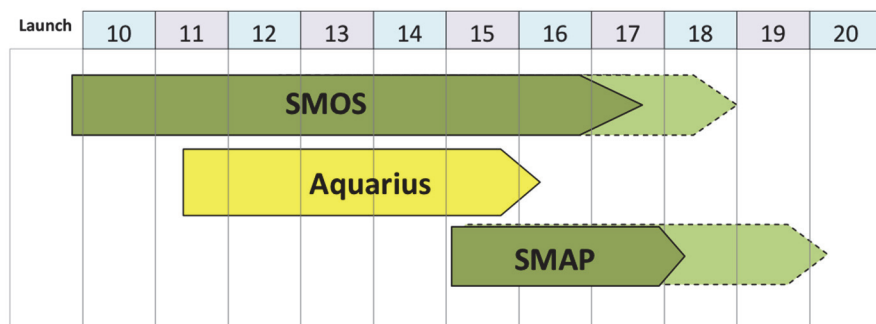


Figure 11.3. Satellite SSS missions.

Basic principles of measuring SSS from space

Measurements from L-band radiometers are used to retrieve SSS using a geophysical model function (Yueh et al., 2014). First, a set of procedures is used to estimate ocean surface brightness temperature (T_B) by removing atmospheric effects (e.g., water vapor, cloud, oxygen absorption) and galactic signals. Three major factors contribute to ocean surface T_B : SSS, SST, and surface roughness. SSS measurements are retrieved after correcting for the effects of SST and surface roughness. Because there is no onboard SST sensor on the L-band satellites, ancillary SST measurements from other satellites are used to remove the SST effect on T_B for all three missions. Surface roughness is generally a more important factor than SST, influencing T_B . Measurements from Aquarius' L-band radar have been very useful in removing the surface roughness effects. SMAP's radar failed after three months into the mission science operation. Therefore, ancillary wind products are used to estimate surface roughness and remove its effect from SMAP's T_B . SMOS does not have an onboard radar, so ancillary winds are also used to remove the effect of surface

roughness on T_B . Splashing due to rain also roughens the ocean surface. Therefore, ancillary rain rate measurements are similarly helpful in removing the related surface roughness effect.

Calibration/validation and satellite SSS error characteristics

Evaluation of satellite SSS measurements are typically performed through comparisons with in situ near-surface salinity measurements obtained from Argo floats, tropical moorings, and ship-based CTD measurements (for level-2 satellite SSS), as well as with gridded maps based on these in situ salinity measurements (for level-3 gridded satellite SSS) (e.g., Tang et al., 2014; Tang et al., 2017). Various analyses of SSS from SMOS, Aquarius, and SMAP have demonstrated that satellite SSS measurements have better accuracy in the tropics and subtropics than at high latitudes. This is because L-band T_B is more sensitive to salinity in warmer waters than in waters colder than 5°C. Two important factors need to be taken into account when assessing the accuracy of satellite SSS using in situ measurements.

(1) Differences in spatiotemporal sampling between satellite and in-situ measurements.

Satellite SSS measurements represent the average SSS values within the satellite footprints (e.g., 33 km for SMOS, 40 km for SMAP, and 100-150 km for Aquarius). In situ measurements are point-wise observations. Evaluation of level-3 satellite SSS measurements is typically performed by “co-locating” in situ measurements within the satellite footprint and a certain time window (e.g., 7-10 days) to gather sufficient samples of in situ data. In regions of high variability (e.g., eddy-rich regions such as the western boundary currents and Antarctic Circumpolar Current, river plumes, tropical regions influenced by instability waves and transient and patchy rain), there could be actual differences between satellite SSS measurements within the footprint and point-wise in situ measurements because the sub-footprint variability is only partially sampled by the point-wise in situ measurements. Likewise, the presence of high-frequency variability can also cause differences between satellite SSS measurements averaged within the selected time window and snapshot in situ measurements. For evaluating level-3 satellite SSS measurements using gridded in situ salinity maps, the uncertainties of the in situ gridded maps due to potentially limited samplings and mapping errors also need to be considered. For example, Lee (2016) showed that in regions of high variability, such as those mentioned previously, the differences between satellite SSS and Argo products are also regions where significant differences exist between two Argo products, reflecting the effect of insufficient sampling by Argo to fully resolve the variability in those regions. Boutin et al. (2016) showed that these regions are in fact associated with substantial variability within satellite footprints as illustrated by ship-based, high-resolution themosalinograph data. Therefore, it is important to note that the differences between satellite SSS (level-2 or level-3) and in situ measurements (individual samples or gridded maps) not only reflect the uncertainties of the satellite SSS measurements, but also the actual differences due to the variances in sampling and mapping. In reality, this is a ubiquitous issue when evaluating satellite measurements using point-wise in situ measurements. It also has implications for the comparison of satellite or in situ measurements with model outputs of different spatial and temporal resolutions.

(2) Effect of near-surface salinity stratification

L-band satellites measure salinity in the top centimeters of the ocean. The shallowest measurement depths for in situ sensors are typically 5 m (for most Argo floats) and 1 m for tropical moorings. Recent measurements of near-surface salinity structures show that there are situations where actual salinity stratification exists above 1 m, especially in the tropics where the effect of transient rain is important (Drucker and Riser, 2014). The shallow, near-surface stratification depends on rain rate and wind speed (which affects vertical mixing) as well as advection by ocean currents. The physics for near-surface stratification is an area of active investigation (Boutin et al., 2016) that has important implications to near-surface vertical mixing and air-sea exchanges. NASA's field experiment Salinity Processes in the Upper Ocean Regional Study-2 (SPURS-2; <https://eurocean3.jpl.nasa.gov/spurs2/index.php>) is an example of recent efforts to understand near-surface salinity stratification and freshwater dispersal.

An international work group, the Satellite and in-situ Salinity Working Group (<http://siss.locean-ipsl.upmc.fr/>), brings the international salinity remote sensing community to further understand the two important issues discussed above. An ongoing project funded by the European Space Agency's SMOS Pilot Mission Exploitation Platform (SMOS Pi-MEP) is compiling various satellite SSS products along with in situ near-surface salinity measurements and ancillary data for validation, analysis, and applications of satellite SSS measurements (<https://pimep-project.odl.bzh/home>).

Scientific accomplishments of the L-band satellite SSS missions

Satellite SSS measurements from the SMOS, Aquarius, and SMAP missions have provided an unprecedented opportunity to map synoptic SSS in the global ocean. These measurements have brought new understanding of various ocean processes such as tropical instability waves (Lee et al., 2012, 2014; Yin et al., 2014), Rossby waves (Menezes et al., 2014), mesoscale eddies (Reul et al., 2014, Melnichenko et al., 2017), salinity fronts (Kao et al., 2014; Yu, 2015), hurricane haline wake (Grodskey et al., 2012), river plume variability (Gierach et al., 2013; Fournier et al., 2016a), and cross-shelf exchanges (Grodskey et al., 2017). They have also enhanced research about the relationship of SSS with climate variability, including research into the El Niño-Southern Oscillation, Indian Ocean Dipole, and Madden-Julian Oscillation (e.g., Grunseich et al., 2013; Guan et al., 2014; Qu and Yu, 2015; Du and Zhang, 2015), and the linkages of the ocean with different elements of the water cycle such as evaporation and precipitation and continental runoff (Yu, 2014; Fournier et al., 2016b).

Additionally, satellite SSS measurements are being used to constrain ocean state estimation and improve seasonal-to-interannual prediction (e.g., Hackert et al., 2014), which are discussed further in the next section. There are also emerging biogeochemical applications of satellite SSS measurements to study ocean's total alkalinity, ocean acidification, and air-sea CO₂ flux (e.g., Land et al., 2015; Fine et al., 2017). The L-band satellites provide complementary measurements to in situ platforms in that they provide global coverage, including the marginal seas and coastal oceans where in situ measurements are often sparse. Satellite SSS observations also capture scales that are

not or inadequately resolved by in situ systems. Examples of these achievements are highlighted in this chapter.

Future challenges and ongoing technology development

The satellite salinity remote sensing community is actively pushing for the continuity and enhancement of satellite SSS observing systems. Enhancement includes two important aspects: (1) increasing spatial resolution to better resolve mesoscale features, which is particularly important to coastal ocean dynamics and biogeochemistry, and (2) improving the quality of satellite SSS observations, especially in high-latitude regions. The larger uncertainties of satellite SSS observation in high-latitude regions is to a large extent a result of the poor sensitivity of L-band T_B to salinity in cold ($< 5^\circ\text{C}$) waters. In order to improve high-latitude satellite SSS measurement quality, ongoing technological developments are focused on combining L- and P-band radiometry. This is because P-band has 2.5-3 times better sensitivity to salinity than L-band for SST lower than 5°C (Fig. 11.4; Lee et al., 2016). The combined L- and P-band radiometry also help improve the uncertainties of seasonal sea ice thickness. Radar measurements of sea ice thickness have relatively large uncertainties for seasonal sea ice. Thus, the combined L/P-band radiometry aims to fill a capability gap in sea ice thickness measurements. More accurate measurements of seasonal sea ice thickness also help improve the retrieval of T_B of the sea ice, which in turn reduce the errors of SSS measurements in marginal ice zones by removing the contamination of SSS signals by leakage of sea ice signal into the field of view of the radiometer over the ocean due to antenna side lobes.

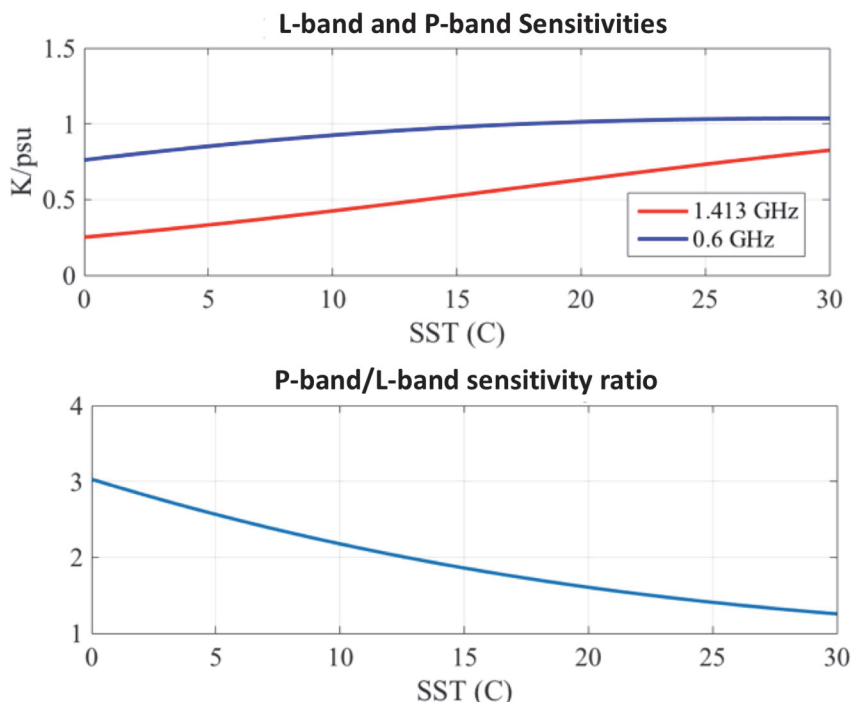


Figure 11.4. L-band and P-band brightness temperature (T_B) sensitivity to SST (upper) and their ratio (lower), showing 2.5-3 times better sensitivity for P-band than L-band for SST $< 5^\circ\text{C}$. After Lee et al. (2016).

Use of Satellite SST and SSS for Constraining Ocean Models

SST data assimilation

Satellite SST products have long been a backbone dataset for most global and regional data assimilation systems due to the relative maturity and operational missions. All current global and regional assimilation systems integrate satellite SST (e.g., see the details under each system in the Ocean Synthesis/Reanalysis Directory <http://icdc.cen.uni-hamburg.de/projekte/easy-init/easy-init-ocean.html> or <http://reanalyses.org/ocean/overview-current-reanalyses>). These include many of the systems under the Global Ocean Data Assimilation (GODAE) OceanView Program.

Assimilation of SST aims to compensate for errors of surface heat flux forcing and to improve the representation of mixed-layer heat budget. For assimilation systems based on the adjoint (or four-dimensional variational) assimilation method such as that used in Estimating the Circulation and Climate of the Ocean (ECCO, <http://www.ecco-group.org>), the assimilation of SST also has the potential to improve surface heat flux estimation (inverse estimation) in combination with other ocean observations that are assimilated. Moreover, the improved estimates of the ocean state can be used to initialize short-term ocean forecasts and seasonal-to-interannual climate prediction. An example of the latter is the assimilation of SST data in JAMSTEC's SINTEX-F coupled ocean-atmosphere model, which demonstrated the positive impacts on the hindcasts of the El Niño-Southern Oscillation and Indian Ocean Dipole (Lou et al., 2005). An example of the encouraging hindcast skill is shown in Fig. 11.5 for Niño3.4 SST anomalies.

Note that SST observations are typically assimilated along with other measurements such as vertical profiles of temperature and salinity from Argo floats, ship-based CTDs, and moorings, as well as sea level anomalies from satellite altimetry to achieve a more comprehensive constraint on the model state. This can avoid misrepresentation of the mixed-layer heat budget through incorrect compensation of different term balance. Additional observational data assimilated typically improve the fidelity of the ocean state estimation (e.g., Fujii et al., 2015).

SSS data assimilation

Even though the satellite SSS data have relatively short records and the products continue to be improved, their values to improve ocean state estimation have been demonstrated. For example, Chakraborty et al. (2014) illustrated the improved representation of equatorial Pacific surface currents through the assimilation of Aquarius SSS data. Toyoda et al. (2015) showed that the assimilation of Aquarius SSS improved the representation of North Pacific mode water characteristics as well as salinity structure near the Maritime Continent, the Amazon plume, the eastern equatorial Pacific, and the Arctic Ocean. Lu et al. (2016) also documented improvements of surface and subsurface salinity fields through assimilation of SMOS SSS data. Köhl et al. (2014) used SMOS SSS to inversely constrain the estimate of the evaporation-precipitation (E-P) forcing field and found positive impacts of the assimilation of SMOS SSS in improving E-P estimates.

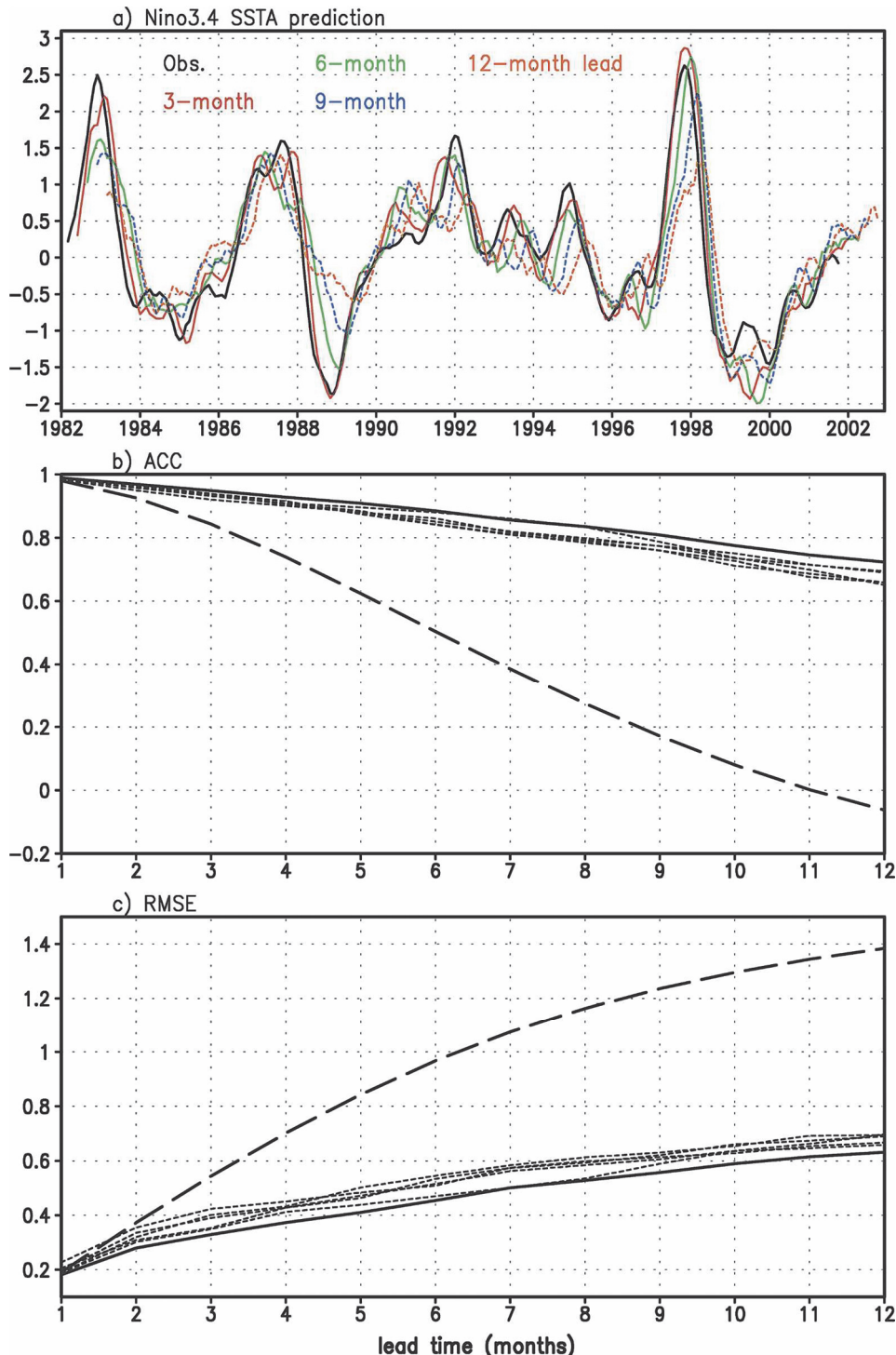


Figure 11.5. (a) Niño-3.4 SST anomalies (5°S – 5°N , $170^{\circ}\text{--}120^{\circ}\text{W}$) based on the NOAA/CDC observations (solid line) and model predictions at three- (red line), six- (green line), nine- (blue line), and 12-month (yellow line) lead times. Results have been smoothed with five-month running mean. (b), (c) ACC (Anomaly Correction Coefficient) scores and RMSEs (Root-Mean Square Errors) of the persistence (long dashed lines), ensemble mean (solid lines), and individual member forecasts (short dashed lines). After Lou et al. (2005).

Satellite SSS data have also been used to improve seasonal-to-interannual prediction. For example, Hacker et al. (2014) demonstrated the positive impacts of Aquarius SSS data assimilation to improve El Niño-Southern Oscillation hindcasts. In that effort, three hindcasts were performed for the period 2011–2014, initialized from three different initial states derived from ocean data assimilation. All three assimilation runs included the subsurface temperature profile data. In the first assimilation, no other data were assimilated. In the second assimilation, in situ salinity data were also assimilated. In the third assimilation, Aquarius SSS were assimilated instead of in situ salinity. The resultant hindcast skills initialized from these three assimilation runs show that the one with Aquarius SSS assimilated had the best hindcast skill for Niño3.4 SST anomalies, both in terms of correlation and root-mean-squared differences from observed Niño3.4 SST anomalies (Fig. 11.6). The improved hindcast skill was attributed to the better sampling of SSS measurements from Aquarius than the in situ measurements, which provides a better constraint on mixed-layer density variation on interannual timescales.

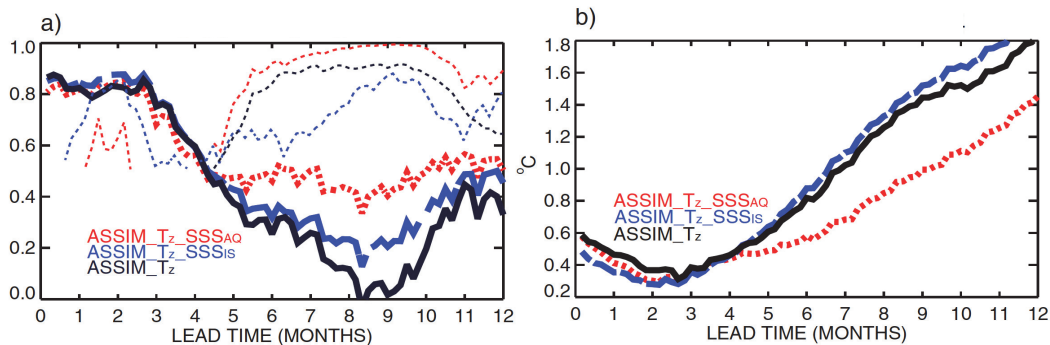


Figure 11.6. Validation of coupled model results for the Aquarius period, August 2011 to February 2014 using (a) correlation and (b) RMS versus observed NINO3 SST anomaly. The solid black curve is initialized using assimilation of subsurface temperature (ASSIM_Tz), the thick dotted red curve from Tz and Aquarius SSS (ASSIM_Tz_SSSAQ) and the dash blue curve from Tz and weekly OI of all available near-surface salinity (ASSIM_Tz_SSSIS). The thin dotted lines show the significance of the differences assuming ASSIM_Tz_SSSAQ (red) and ASSIM_Tz_SSSIS (blue) are greater than ASSIM_Tz and ASSIM_Tz_SSSAQ is greater than ASSIM_Tz_SSSIS (black) using the Fisher Z test. Note that Fisher Z test is undefined (thus missing) when this condition fails.

Other ongoing efforts to employ satellite SSS assimilation include those by the Estimating the Circulation and Climate of the Ocean consortium (<http://www.ecco-group.org>), the NASA Goddard Space Flight Center, NOAA's Joint Center for Satellite Data Assimilation, the UK Meteorology Office, the French Mercator Ocean, and the Chinese National Marine Environmental Forecasting Center. In particular, the UK Meteorology Office and Mercator Ocean are conducting an observing system experiment to test the impacts of satellite SSS data assimilation on simulating the 2015–16 El Niño (<https://www.godae-oceanview.org/projects/smos-nino15>), an effort funded by the European Space Agency. The project is also part of the GODAE OceanView's Observing System Evaluation Task Team effort.

The fidelity of ocean models in presenting salinity has been not as good as for presenting temperature. There are three major contributing factors: (1) uncertainties of E-P forcing, (2) lack of

discharge estimates for many rivers around the world, and (3) the lack of historical salinity observations (including SSS).

E-P is an important forcing for modelled SSS. In ocean models, E-P forcing is typically obtained from atmospheric models or analysis/reanalysis products that are subject to relatively large uncertainties, especially in terms of their global net balance. The errors in E-P forcing cause ocean models to deviate or drift away from reality. To alleviate this, a common practice in ocean modeling is to relax modelled SSS towards a seasonal climatology derived from historical in situ measurements (this is a crude way to compensate for the error of E-P forcing). In fact, a similar approach was used for SSTs (i.e., relaxing toward seasonal climatology) before the sustained development and improvement of the operational satellite SST observing system. Relaxation of modelled SSS to seasonal climatology tends to reduce the amplitudes of the non-seasonal SSS signals in ocean models. The development of the Argo system has provided broad-scale SSS measurements in the past decade. However, the Argo array is not global (it has limited to no coverage in many marginal seas, coastal oceans, and polar oceans). Satellite SSS observations thus provide a potentially important database for constraining ocean models to correct for errors in E-P and model representation of ocean dynamics.

In coastal oceans and marginal seas significantly affected by rivers, freshwater input from river discharge is an important forcing factor for SSS. However, due to the lack of accurate observations for the discharges of many rivers around the world (especially for interannually varying time series and near real-time data availability), a common practice in ocean models is to use estimates of seasonal climatology for river discharges (e.g., those from Dai and Trenberth, 2002 or other sources). SSS variations near river mouths in ocean models typically have little interannual variations even though satellite SSS data have revealed substantial interannual variations near some river mouths (e.g., Grodsky et al., 2014; Fournier et al., 2016a).

Therefore, the assimilation of satellite SSS data, especially in coastal oceans and marginal seas where in situ data tend to be sparse (or non-existent), can help improve the representation of salinity structure in ocean models. The improvement of salinity in these regions have significant implications to marine biogeochemistry.

Treatment of biases in observations and models in assimilation

An important issue in assimilating SST and SSS observations are potential biases in the data. Some assimilation schemes assume that the data are un-biased whereas in reality biases do exist in the data. For example, there are relative biases between SST datasets based on infrared and passive microwave sensors. Significant biases still exist in satellite SSS measurements. Biases can limit the effectiveness of the data in constraining the model representation of the temporal variability, especially when (and where) the magnitude of the biases are not small comparing to the magnitude of the temporal variability. Bias correction schemes have been employed in some assimilation systems to alleviate this issue. An example is the UK Meteorology Office's FOAM-NEMOVAR system (<https://www.metoffice.gov.uk/binaries/content/assets/mohippo/pdf/t/e/frtr578.pdf>) where bias correction was applied to the SST data by referencing the biased SST data to a reference set of

observations that are known or assumed to be unbiased, similar to the procedure applied by Martin et al. (2007). Biases in observational data are not necessarily unique to SST and SSS and the related assimilation, but present in other observations as well.

Model biases also reduce the effectiveness of the assimilation to constrain the temporal variability in the model using temporal signals in the data. This is because the assimilation works hard to correct the model biases using the observations, thus limiting the influence of the temporal variability in the observations to constrain the temporal variability of the model. A widely-used approach to tackle this issue is to perform anomaly data assimilation, i.e., only use the temporal variability in the observations to constrain the counterpart in the model (e.g., Hackert et al., 2014). In the ECCO estimation system, the time mean state and temporal anomalies of the model are constrained by the corresponding values of the observations, respectively, by separating the constraint on the time mean and temporal anomalies separately in the cost function. Moreover, the control variables (e.g., surface forcing) are also separated into time mean and temporal anomalies, weighted by the respective a priori uncertainties.

Importance of understanding uncertainty characteristics of SST and SSS observations

It is also important to understand the uncertainty characteristics of the SST and SSS observations that assimilated into models beyond just the biases. There are three important sources of uncertainties for satellite SST observations: (1) effect of clouds on SST from infrared sensors, (2) ability to resolve diurnal variability, and (3) larger uncertainties in the Arctic Ocean. In particular, the GHRSST Project has identified the latter to be an important issue in terms of improving satellite SST data. The larger discrepancies among satellite SST products in the Arctic Ocean and differences from in situ SST data were reported by (Castro et al., 2016), who found large differences of various level-4, blended GHRSST products in the Arctic Ocean. The GHRSST Multi-Product Ensemble project produces median and standard deviation (Fig. 11.7) based on a dozen GHRSST products (<https://www.ghrsst.org/latest-sst-map/>) for the global ocean. The GHRSST Multi-Product Ensemble provides important resources to understand the consistency and uncertainties of the GHRSST products.

As discussed in earlier, L-band satellite SSS data generally have larger uncertainties in high-latitude oceans. This is in large part due to the poor sensitivity of L-band T_Bto SSS in cold-water (<5 °C) environment. The larger uncertainty of SST (an ancillary data used in SSS retrieval) also contribute. As an example, the standard deviation values for various spatial scales between monthly, level-3 Aquarius Version-4 SSS and the 5 m salinity from an Argo-based monthly gridded product from the Scripps Institution of Oceanography is shown in Fig. 11.8 (Lee, 2016). The discrepancies between the Aquarius SSS and the Argo product in high-latitude oceans are larger than those at lower latitudes by a few times. Similarly, SMOS and SMAP SSS products have larger discrepancies with Argo products (not shown). This error structure is helpful to the assimilation of Aquarius SSS data.

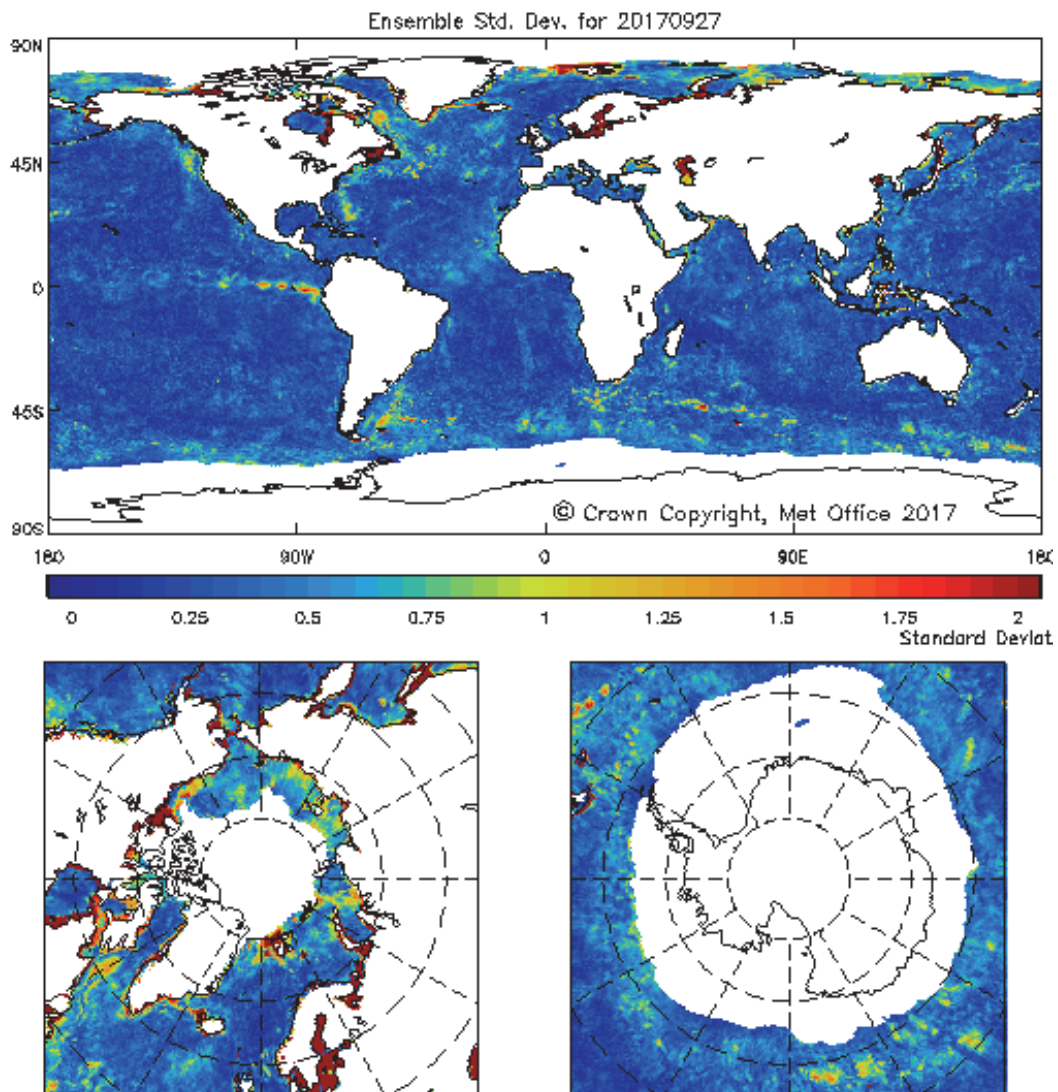


Figure 11.7. The spread among 11 SST products on 27 September 2017 (from <https://www.ghrsst.org/latest-sst-map>) as part of GHRSSST's Multi-Product Ensemble comparison project, which is from the Copernicus Marine Environment Monitoring Service. © Crown copyright, Met Office.

It is important to note that the discrepancies between satellite SSS and the in situ-based gridded near-surface salinity products cannot be entirely contributed to the errors of the satellite SSS. The sampling differences between satellite SSS measurements (averages with the satellite footprint) and in situ (point-wise) measurements as well as the mapping errors also contribute. The nominal density of the Argo array is one profile $3^\circ \times 3^\circ$ at 10-day intervals. In areas with strong currents and divergence, the sampling of the Argo array may further reduce. As discussed earlier, in regions with high-frequency and small-scale variability, there will be larger sampling errors from Argo (e.g., insufficient sampling to accurately represent monthly averages on $1^\circ \times 1^\circ$ or $3^\circ \times 3^\circ$ scales. In fact, Figs. 11.8d and 11.8e illustrate relatively large standard deviation values between the Argo-Scripps product and that from University of Hawaii in regions of strong variability (e.g., tropical rain bands,

river plumes, western boundary currents, Antarctic Circumpolar Current, etc.). The white-out areas in the third column of Fig. 11.8 show the locations where the differences between Argo-Scripps and Argo-University of Hawaii are larger than those between Aquarius and Argo-Scripps. If one excludes these areas, the areal average standard deviation between Aquarius and Argo is significantly smaller (the red values in the third column). The relative uncertainties of satellite and in situ SSS data due to the sampling differences need to be considered in assimilating salinity data in models with various resolutions. Even though the example above is for gridded satellite SSS and Argo products, the issue also applies for level-2 satellite SSS and individual in situ salinity measurements, as discussed earlier in this chapter.

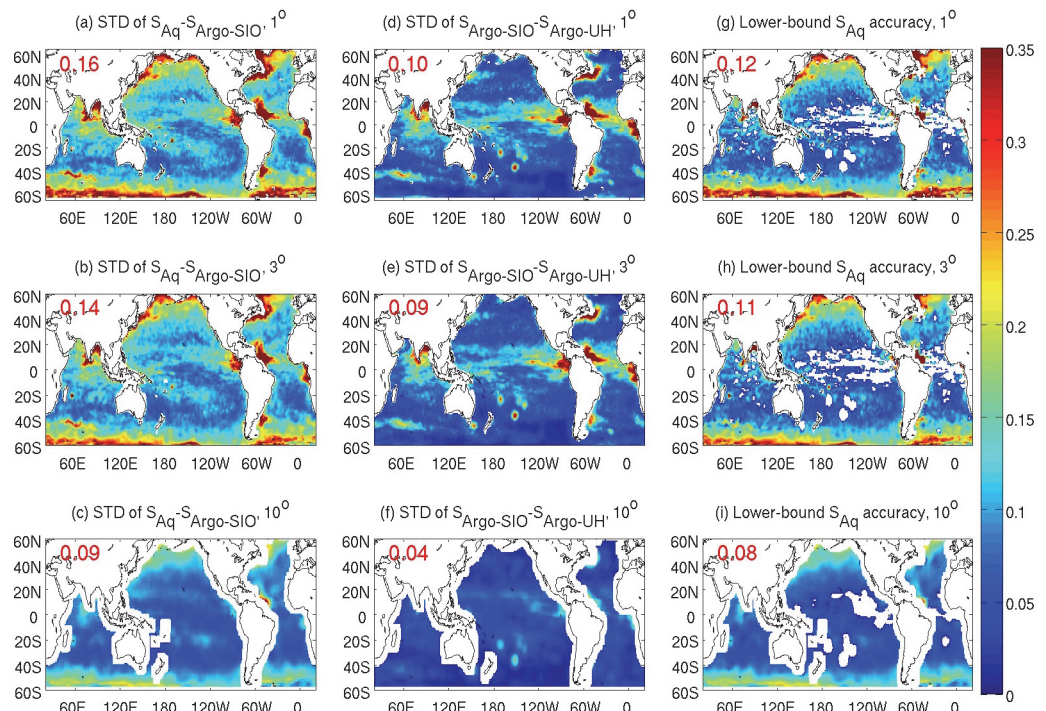


Figure 11.8. Standard deviation of SSS differences between Aquarius and Argo-Scripps on (a) $1^\circ \times 1^\circ$, (b) $3^\circ \times 3^\circ$, and (c) $10^\circ \times 10^\circ$ scales and between (d–f) Argo-Scripps and Argo-University of Hawaii on these scales. The values in Figs. 1a–1c represent upper-bound Aquarius SSS accuracies. (g–i) The estimated lower-bound Aquarius SSS accuracies obtained by removing the variance at each location in Figs. 1d–1f from that in Figs. 1a–1c then took the square root. The white-out mid-ocean grid points in Figs. 1g–1i indicate where the discrepancies between the two Argo products are larger than those between Aquarius and Argo. The red numbers indicate the respective global averages of standard deviation. After Lee (2016).

Acknowledgments

This research was carried out in part at the Jet Propulsion Laboratory (JPL), California Institute of Technology, under a contract with NASA, supported by NASA Physical Oceanography Program.

References

- Bjerknes, J., 1969: Atmospheric teleconnections from the equatorial Pacific. *Mon. We. Rev.*, 97, 163-172.
- Boutin, J., et al., 2016: Satellite and in situ salinity: understanding near surface stratification and sub-footprint variability. *Bull. Amer. Meteorol. Soc.*, Vol.97, Issue 8, 1391-+, DOI: 10.1175/BAMS-D-15-00032.1.
- Casey, K. S., Brandon, T. B., Cornillon, P., and Evans, R., 2010: The past, present, and future of the AVHRR Pathfinder SST program. In *Oceanography from space* (pp. 273-287). Springer Netherlands.
- Castro, S.L., G.A. Wick, and M. Steele, 2016: Validation of satellite sea surface temperature analyses in the Beaufort Sea using UpTempO buoys. *Remote Sensing of Environment*, vol. 187, pp. 458-475.
- Chakraborty, A., Kumar, R., Basu, S., and Sharma, R. (2015a). Improving Ocean State by Assimilating SARAL/AltiKa Derived Sea Level and Other Satellite-Derived Data in MITGCM, *Mar. Geod.*, 38 (Sup 1), 328-338, doi: 10.1080/01490419.2014.1002142.
- Chelton, D. B., S. K. Esbensen, M. G. Schlax, N. Thum, M. H. Freilich, F. J. Wentz, C. L. Gentemann, M. J. McPhaden, and P. S. Schopf, 2001: Observations of coupling between surface wind stress and sea surface temperature in the eastern tropical Pacific, *Journal of Climate*, 14(7), 1479-1498.
- Donlon, C. J., Minnett, P. J., Gentemann, C., Nightingale, T. J., Barton, I. J., Ward, B., & Murray, M. J., 2002: Toward improved validation of satellite sea surface skin temperature measurements for climate research. *Journal of Climate*, 15(4), 353-369.
- Donlon, C., Rayner, N., Robinson, I., Poulter, D. J. S., Casey, K. S., Vazquez-Cuervo, J., and May, D., 2007: The global ocean data assimilation experiment high-resolution sea surface temperature pilot project. *Bulletin of the American Meteorological Society*, 88(8), 1197-1213.
- Droghei, R., B. Buongiorno Nardelli, and R. Santoleri, 2016: Combining in-situ and satellite observations to retrieve salinity and density at the ocean surface, *J. Atmos. Ocean. Technol.*, 33, 1211-1223, doi:10.1175/JTECH-D-15-0194.1.
- Drucker, R., & Riser, S. C., 2014: Validation of Aquarius sea surface salinity with Argo: Analysis of error due to depth of measurement and vertical salinity stratification. *Journal of Geophysical Research: Oceans*, 119(7), 4626-4637.
- Du, Y. and Zhang, Y., 2015: Satellite and Argo Observed Surface Salinity Variations in the Tropical Indian Ocean and Their Association with the Indian Ocean Dipole Mode, *J. Climate*, 28 (2), 695-713, doi: 10.1175/JCLI-D-14-00435.1.
- Entekhabi, D. et al., 2014: SMAP handbook soil moisture active passive: Mapping soil moisture and freeze/thaw from space, JPL CL14-2285, Jet Propulsion Laboratory, Pasadena, CA.
- Fine, R.A., Willey, D.A., and Millero, F.J., 2017: Global Variability and Changes in Ocean Total Alkalinity from Aquarius Satellite Data, *Geophys. Res. Lett.*, 44 (1), 261-267, doi: 10.1002/2016GL071712.
- Fournier, S., T. Lee, and M. Gierach, 2016a: Seasonal and interannual variations of sea surface salinity associated with the Mississippi River plume observed by SMOS and Aquarius. *Remote Sensing. Environ.* 180, 431-439.
- Fournier, S., J.T. Reager, and T. Lee et al., 2016b: SMAP observes flooding from land to sea: The Texas event of 2015. *Geophys. Res. Lett.*, 43, 10.1002/2016GL068822.
- Gentemann, C. L., Wentz, F. J., Mears, C. A., & Smith, D. K., 2004: In situ validation of Tropical Rainfall Measuring Mission microwave sea surface temperatures. *Journal of Geophysical Research: Oceans*, 109(C4).
- Gentemann, C. L., 2014: Three-way validation of MODIS and AMSR-E sea surface temperatures. *Journal of Geophysical Research: Oceans*, 119(4), 2583-2598.
- Gentemann, C. L., and Hilburn, K. A., 2015: In situ validation of sea surface temperatures from the GCOM-W1 AMSR2 RSS calibrated brightness temperatures. *Journal of Geophysical Research: Oceans*, 120(5), 3567-3585.
- Gierach, M.M., J. Vazquez, T. Lee, and V. Tsontos, 2013: Aquarius and SMOS detect effects of an extreme Mississippi River flooding event in the Gulf of Mexico. *Geophys. Res. Lett.*, 40, doi:10.1002/grl.50995.
- Grodsky, S., N. Reul, G.S.E., Lagerloef, et al. 2012: Haline Hurricane Wake in the Amazon/Orinoco Plume: AQUARIUS/SAC-D and SMOS Observations, *Geophys. Res. Lett.*, 39 (20), L20603, doi:10.1029/2012GL053335.
- Grodsky, S.A., Reul, N., Chapron, B., Carton, J.A., and Bryan, F.O., 2017: Interannual Surface Salinity in Northwest Atlantic Shelf, *J. Geophys. Res.-Oceans*, 122 (5), 3638-3659, doi: 10.1002/2016JC012580.
- Grodsky, S.A., Reverdin, G., Carton, J.A., and Coles, V.J., 2014b. Year-to-Year Salinity Changes in the Amazon Plume: Contrasting 2011 and 2012 Aquarius/SAC-D and SMOS Satellite Data, *Remote Sens. Environ.*, 140, 14-22, doi: 10.1016/j.rse.2013.08.033.
- Grunseich, G., Subrahmanyam, B., and Wang, B., 2013: The Madden-Julian Oscillation Detected in Aquarius Salinity Observations, *Geophys. Res. Lett.*, 40 (20), 5461-5466, doi:10.1002/2013GL058173.

- Guerrero, R.A., Piola, A.R., Fenco, H., Matano, R.P., Combes, V., Chao, Y., James, C., Palma, E.D., Saraceno, M., and Strub, P.T., 2014: The Salinity Signature of the Cross-Shelf Exchanges in the Southwestern Atlantic Ocean: Satellite Observations, *J. Geophys. Res.-Oceans*, 119 (11), 7794–7810, doi: 10.1002/2014JC010113.
- Guan, B., T., Lee, T., D. Halkides, et al., 2014: Aquarius surface salinity and the Madden-Julian Oscillation: the role of salinity in surface layer density and potential energy, *Geophys. Res. Lett.*, 41 (8), 2858–2869, doi:10.1002/2014GL059704.
- Hackert, E., A. J. Busalacchi, and J. Ballabrera-Poy, 2014: Impact of Aquarius sea surface salinity observations on coupled forecasts for the tropical Indo-Pacific Ocean, *J. Geophys. Res. Oceans*, 119, 4045–4067, doi:10.1002/2013JC009697.
- Kao, H.Y. and G.S.E. Lagerloef, G.S.E., 2015: Salinity Fronts in the Tropical Pacific Ocean, *J. Geophys. Res.-Oceans*, 120 (2), 1096–1106, doi:10.1002/2014JC010114.
- Köhl, A., M. Sena Martins, and D. Stammer, 2014: Impact of assimilating surface salinity from SMOS on ocean circulation estimates, *J. Geophys. Res. Oceans*, 119, 5449–5464, doi:10.1002/2014JC010040.
- Kumar A., and Hoerling M.P., 1998: Annual cycle of Pacific/North American seasonal predictability associated with different phases of ENSO. *Journal of Climate* 11: 3295–3308.
- Lagerloef, G., and J. Font, 2010: SMOS and Aquarius/SAC-D Missions: The Era of Spaceborne Salinity Measurements is About to Begin, *Oceanography from Space*, 35–58, doi: 10.1007/978-90-481-8681-5_3.
- Lagerloef, G., S.H. Yueh, and J. Piepmeier, 2013: Review & Forecast: NASA's Aquarius Mission Provides New Ocean View, *Sea Technol.*, 54 (1), 26–29.
- Land, P.E., Shutler, J.D., Findlay, H.S., Girard-Ardhuin, F., Sabia, R., Reul, N., Piolle, J.-F., Chapron, B., Quilfen, Y., Salisbury, J., Vandemark, D., Bellerby, R., and Bhadury, P., 2015: Salinity from Space Unlocks Satellite-Based Assessment of Ocean Acidification, *Environ. Sci. Technol.*, 49 (4), 1987–1994, doi:10.1021/es504849s.
- Lee, T., G. Lagerloef, M. M. Gierach, H.-Y. Kao, S. Yueh, and K. Dohan, 2012: Aquarius reveals salinity structure of tropical instability waves, *Geophys. Res. Lett.*, 39, L12610, doi:10.1029/2012GL052232.
- Lee, T., G. Lagerloef, H.-Y. Kao, M.J. McPhaden, J. Willis, and M.M. Gierach, 2014: The influence of salinity on tropical Atlantic instability waves. *J. Geophys. Res.*, 10.1002/2014JC010100.
- Lee, T., 2016: Consistency of Aquarius sea surface salinity with Argo products on various spatial and temporal scales. *Geophys. Res. Lett.*, 43, 10.1002/2016GL068822.
- Lee, T et al., 2016: Linkages of salinity with ocean circulation, water cycle, and climate variability. Community white paper in response to Request for Information #2 by the US National Research Council Decadal Survey for Earth Science and Applications from Space 2017–2027. http://surveygizmoresponseuploads.s3.amazonaws.com/fileuploads/15647/2604456/107-1abc9aa1a37ab7e77d91d86598954a50_LeeTong.pdf
- Lindstrom, E., R. Lukas, R. Fine, et al. 1987: The western equatorial Pacific Ocean circulation study, *Nature*, 330, 533–538.
- Llewellyn-Jones, D., Edwards, M. C., Mutlow, C. T., Birks, A. R., Barton, I. J., and Tait, H., 2001: AATSR: Global-change and surface-temperature measurements from Envisat. *ESA bulletin*, 105(10-21), 25.
- Lu, Z., L. Cheng, J. Zhu, and R. Lin, 2016: The complementary role of SMOS sea surface salinity observations for estimating global ocean salinity state, *J. Geophys. Res. Oceans*, 121, 3672–3691, doi:10.1002/2015JC011480.
- Luo, J.-J. et al., 2005: Seasonal Climate Predictability in a coupled OAGCM using different approach for Ensemble Forecasts. *J. Climate*, 18, 4474–4497. doi:10.1175/JCLI3526.1.
- Martin, M., J.A. Hines, and M. J. Bell, 2007: Data assimilation in the foam operational short-range ocean forecasting system: a description of the scheme and its impact. *Q. J. Roy. Meteorol. Soc.*, 133:981–995, 2007.
- Melnichenko, O., A. Amores, N. Maximenko, et al., 2017: Signature of Mesoscale Eddies in Satellite Sea Surface Salinity Data, *J. Geophys. Res.-Oceans*, 122 (2), 1416–1424, doi:10.1002/2016JC012420.
- Menezes, V.V., M.L. Vianna, and H.E. Phillips, 2014: Aquarius Sea Surface Salinity in the South Indian Ocean: Revealing Annual-Period Planetary Waves, *J. Geophys. Res.-Oceans*, 119 (6), 3883–3908, doi:10.1002/2014JC009935.
- Nardelli, B., R. Droghei, and R. Santoleri, 2016: Multi-dimensional interpolation of SMOS sea surface salinity with surface temperature and in situ salinity data, *Remote Sens. Environ.*, 180, 392–402, doi:10.1016/j.rse.2015.12.052.
- O'Carroll, A. G., Eyre, J. R., & Saunders, R. W., 2008: Three-way error analysis between AATSR, AMSR-E, and in situ sea surface temperature observations. *Journal of Atmospheric and Oceanic Technology*, 25(7), 1197–1207.

- Olmedo, E., Martínez, J., Umbert, M., Hoareau, N., Portabella, M., Ballabrera, J., Turiel, A., 2016: Improving time and space resolution of SMOS salinity maps using multifractal fusion. *Remote Sensing of Environment* 180, 246-263, doi:10.1016/j.rse.2016.02.038.
- Qu, T.D. and J.-Y. Yu, 2014: ENSO Indices from Sea Surface Salinity Observed by Aquarius and Argo, *J. Oceanogr.*, 70 (4), 367-375, doi:10.1007/s10872-014-0238-4.
- Reul, N., J. Tenerelli, B. Chapron, D. Vandemark, Y. Quilfen, and Y. Kerr, 2012: SMOS satellite L-band radiometer: A new capability for ocean surface remote sensing in hurricanes, *J. Geophys. Res.*, 117, C02006, doi:10.1029/2011JC007474.
- Reul, N., B. Chapron, T. Lee, C. Donlon, J. Boutin, G. Alory, 2014: Sea surface salinity structure of the meandering Gulf Stream revealed by SMOS sensor. *Geophys. Res. Lett.*, DOI: 10.1002/2014GL059215.
- Reynolds, R. W., 1993: Impact of Mount Pinatubo aerosols on satellite-derived sea surface temperatures. *Journal of climate*, 6(4), 768-774.
- Reynolds, R. W., T. M. Smith, C. Liu, et al., 2007: Daily high-resolution-blended analyses for sea surface temperature, *J. Clim.*, 20, 5473–5496, doi:10.1175/2007JCLI1824.1.
- Sprintall, J., and M. Tomczak (1992), Evidence of the barrier layer in the surface layer of the tropics, *J. Geophys. Res.*, 97(C5), 7305-7316.
- Tang, W., Yueh, S. H., Fore, A. G., and Hayashi, A., 2014: Validation of Aquarius sea surface salinity with in situ measurements from Argo floats and moored buoys. *Journal of Geophysical Research: Oceans*, 119(9), 6171-6189.
- Tang, W., A. Fore, S. Yueh, T. Lee, A. Hayashi, A. Sanchez-Franks, B. King, D. Baranowski, and J. Martinez, 2017: Validating SMAP SSS with in-situ measurements. *Remote Sensing Environ.*, doi:10.1016/j.rse.2017.08.021.
- Toyoda, T., Fujii, Y., Kuragano, T., Matthews, J.P., Abe, H., Ebuchi, N., Usui, N., Ogawa, K., and Kamachi, M., 2015: Improvements to a Global Ocean Data Assimilation System Through the Incorporation of Aquarius Surface Salinity Data, *Q. J. Roy. Meteor. Soc.*, 141 (692), 2750-2759, doi: 10.1002/qj.2561.
- Umbert, M., N. Hoareau, A. Turiel, and J. Ballabrera-Poy, 2013: New blending algorithm to synergize ocean variables: The case of SMOS sea surface salinity maps, *Remote Sens. Environ.*, doi:10.1016/j.rse.2013.09.018.
- Xie, P., T. Boyer, E. Bayler, et al., 2014: An In Situ-satellite Blended Analysis of Global Sea Surface Salinity, *J. Geophys. Res.-Oceans*, 119 (9), 6140-6160, doi:10.1002/2014JC010046.
- Yin, X., J. Boutin, and G. Reverdin, et al., 2014: SMOS sea surface salinity signals of tropical instability waves. *J. Geophys. Res.*, 119, 7811–7826, doi:10.1002/2014JC009960.
- Yu, L., 2014: Coherent Evidence from Aquarius and Argo for the Existence of a Shallow Low-salinity Convergence Zone Beneath the Pacific ITCZ, *J. Geophys. Res.-Oceans*, 119 (11), 7625-7644, doi: 10.1002/2014JC010030.
- Yu, L., 2015: Sea-surface Salinity Fronts and Associated Salinity Minimum Zones in the Tropical Ocean, *J. Geophys. Res.-Oceans*, 120 (6), 4205-4225, doi:10.1002/2015JC010790.
- Yueh, S., Tang, W., Fore, A., Hayashi, A., Song, Y. T., and Lagerloef, G., 2014: Aquarius geophysical model function and combined active passive algorithm for ocean surface salinity and wind retrieval. *Journal of Geophysical Research: Oceans*, 119(8), 5360-5379.

